Comparative Effects of the Endogenous Agonist Glucagon-Like Peptide-1 (GLP-1)-(7-36) Amide and the Small-Molecule Ago-Allosteric Agent "Compound 2" at the GLP-1 Receptor

Karen Coopman, Yan Huang, Neil Johnston, Sophie J. Bradley, Graeme F. Wilkinson, and Gary B. Willars

Department of Cell Physiology and Pharmacology, University of Leicester, Leicester, United Kingdom (K.C., Y.H., N.J., S.J.B., G.B.W.); and Biological Chemistry, Discovery Enabling Capabilities and Sciences, AstraZeneca, Alderley Park, Macclesfield, United Kingdom (G.F.W.)

ABSTRACT

Glucagon-like peptide-1 (GLP-1) mediates antidiabetogenic effects through the GLP-1 receptor (GLP-1R), which is targeted for the treatment of type 2 diabetes. Small-molecule GLP-1R agonists have been sought due to difficulties with peptide therapeutics. Recently, 6,7-dichloro-2-methylsulfonyl-3-*N-tert*-butylaminoquinoxaline (compound 2) has been described as a GLP-1R allosteric modulator and agonist. Using human embryonic kidney-293 cells expressing human GLP-1Rs, we extended this work to consider the impact of compound 2 on G protein activation, Ca^{2+} signaling and receptor internalization and particularly to compare compound 2 and GLP-1 across a range of functional assays in intact cells. GLP-1 and compound 2 activated $G\alpha_s$ in cell membranes and increased cellular cAMP in intact cells, with compound 2 being a partial and almost full agonist, respectively. GLP-1 increased intracellular $[Ca^{2+}]$ by release from intracellular stores, which was mimicked by compound 2, with slower kinetics. In either intact cells or membranes, the orthosteric antagonist exendin-(9-39), inhibited GLP-1 cAMP generation but increased the efficacy of compound 2. GLP-1 internalized enhanced green fluorescent protein-tagged GLP-1Rs, but the speed and magnitude evoked by compound 2 were less. Exendin-(9-39) inhibited internalization by GLP-1 and also surprisingly that by compound 2. Compound 2 displays GLP-1R agonism consistent with action at an allosteric site, although an orthosteric antagonist increased its efficacy on cAMP and blocked compound 2-mediated receptor internalization. Full assessment of the properties of compound 2 was potentially hampered by damaging effects that were particularly manifest in either longer term assays with intact cells or in acute assays with membranes.

Introduction

Glucagon-like peptide-1 (GLP-1) is a potent modulator of insulin secretion that is released by L cells of the intestine in response to nutrient ingestion (Reimann et al., 2006). It is generated from proglucagon and exists as several truncated versions of the full-length peptide, with the predominantly active form being GLP-1-(7-36) amide (Orskov et al., 1994). GLP-1 exerts its actions through the GLP-1 receptor (GLP-1R), a family B G protein-coupled receptor. The GLP-1R is primarily coupled to $G\alpha_s$ and thereby mediates its effects through the generation of cAMP and its downstream targets, although coupling to $G\alpha_{i/o}$ and $G\alpha_{q/11}$ has been reported previously (Montrose-Rafizadeh et al., 1999; Hällbrink et al., 2001; Bavec et al., 2003). It is largely as a consequence of its ability to promote glucose-dependent insulin release from pancreatic β cells (Holst et al., 1987; Holz et al., 1993) that it is an established target for the treatment of type 2 diabetes. In addition, GLP-1 contributes to appropriate glucose homeostasis by increasing insulin biosynthesis, suppressing glucagon secretion, stimulating β-cell mass, and suppressing appetite (Baggio and Drucker, 2007; Doyle and Egan, 2007; Holst, 2007). In vivo, GLP-1 has a plasma half-life of only 1 to 2 min because it is subject to rapid

ABBREVIATIONS: GLP-1, glucagon-like peptide-1; GLP-1R, glucagon-like peptide-1 receptor; compound 2, 6,7-dichloro-2-methylsulfonyl-3-*N-tert*-butylaminoquinoxaline; h, human; HEK, human embryonic kidney; EGFP, enhanced green fluorescent protein; AM, acetoxymethyl ester; U73122, 1-[6-[[17β-methoxyestra-1,3,5(10)-trien-17-yl]amino]hexyl]-1*H*-pyrrole-2,5-dione; U73343, 1-[6-[[17β-3-methoxyestra-1,3,5(10)-trien-17-yl]amino]hexyl]-2,5-pyrrolidine-dione; GTPγS, guanosine 5′-*O*-(3-thio)triphosphate; CTX, cholera toxin; BSA, bovine serum albumin; KHB, Krebs-HEPES buffer; IBMX, isobutylmethylxanthine; DMSO, dimethyl sulfoxide; PKA, protein kinase A.

proteolytic degradation, particularly by the serine protease dipeptidyl peptidase-IV, which cleaves the two N-terminal amino acid residues and renders the molecule biologically inactive (Mentlein et al., 1993; Kieffer et al., 1995).

The proteolytic degradation of GLP-1 presents considerable difficulties for therapeutic use, and a range of dipeptidyl peptidase-IV-resistant analogs of GLP-1 such as liraglutide (NN2211; Novo Nordisk, Copenhagen, Denmark), CJC-1131 (ConjuChem, Montreal, QC, Canada), and exenatide (exendin-4, AC2993; Amylin Pharmaceuticals/Eli Lilly & Co., Indianapolis, IN) (see Meier and Nauck, 2005 for review) have been developed. Although these agents and their derivatives have therapeutic potential, difficulties associated with the long-term administration of peptides have driven the search for small-molecule, orally active agonists of the GLP-1R. Recently, an exciting development has been the identification of a small-molecule ligand of the GLP-1R, which not only increases the affinity of the GLP-1R for GLP-1 but also is an agonist in its own right (Knudsen et al., 2007). This ago-allosteric agent, 6,7-dichloro-2-methylsulfonyl-3-N-*tert*-butylaminoquinoxaline (compound 2), stimulates cAMP production in membranes generated from baby hamster kidney cells expressing the human GLP-1R (hGLP-1R), albeit with a bell-shaped concentration-response curve, and also potentiates glucose-induced insulin release from pancreatic islets isolated from rodents. In the present study, we have generated HEK-293 cell lines expressing either the hGLP-1R or this receptor with a C-terminal enhanced green fluorescent protein (EGFP) epitope-tag to further characterize signaling by compound 2, particularly to directly compare its actions with those of the major endogenous ligand GLP-1-(7-36) amide and to examine potential interactions between compound 2 and this orthosteric ligand.

Materials and Methods

Materials

All tissue culture plasticware was purchased from Nunc (VWR International, Lutterworth, UK). Media, fetal bovine serum, Lipofectamine 2000, oligonucleotides, Geneticin (G418), fluo-4-acetoxymethyl ester (fluo-4-AM), Pluronic acid F-127, and hygromycin B were from Invitrogen (Paisley, UK). GLP-1-(7-36) amide and exendin-(9-39) were purchased from Bachem (Weil am Rhein, Germany), and compound 2 was synthesized at AstraZeneca UK (Alderley Edge, UK) based on a previously reported method (Knudsen et al., 2007). U73122 and U73343 (Bleasdale et al., 1990) were from Enzo Life Sciences (Exeter, UK). Protein A-Sepharose beads, [2,8-^{3}H]adenosine 3',5'-cyclic phosphate, ammonium salt ([^{3}H]cAMP; 40 Ci/mmol), and [^{35}S]GTPγS (1048 Ci/mmol) were obtained from GE Healthcare (Little Chalfont, Buckinghamshire, UK). Emulsifier Safe scintillation fluid, Whatman GF/B glass fiber filters, and ^{125}I-GLP-1-(7-36) amide (2000 Ci/mmol) were purchased from PerkinElmer Life and Analytical Sciences Ltd. (Buckinghamshire, UK). Antibodies against the Gα_s and G$\alpha_{i/o/t/z/gust}$ protein subunits were purchased from Santa Cruz Biotechnology, Inc. (Santa Cruz, CA), and a monoclonal G$\alpha_{q/11}$ antibody was generated (Bundey and Nahorski, 2001) by Genosys Biotechnologies (Pampisford, UK) by inoculation of rabbits with the decapeptide (sequence QLNLKEYNLV), which is common to the C terminus of both Gα_q and Gα_{11}. The pEGFP-N1 plasmid encoding EGFP for C-terminal tagging of the GLP-1R was from Clontech Laboratories (Saint-Germain-en-Laye, France). Restriction endonucleases were purchased from New England Biolabs (Hitchin, UK). DNA plasmid preparation and DNA gel extraction kits were from QIAGEN (Crawley, UK), and agarose powder was from

BiozymT BV (Landgraaf, The Netherlands). All other chemicals including pertussis toxin and cholera toxin (CTX) were purchased from Sigma-Aldrich (Gillingham, UK).

Cell Culture and Generation of Cell Lines with Stable Expression of hGLP-1Rs

HEK-Flp-In cells, wild-type HEK-293 cells, HEK-Flp-In cells with stable expression of the hGLP-1R (HEK-GLP-1R), or HEK-293 cells with stable expression of a C-terminal EGFP-tagged hGLP-1R (HEK-GLP-1R-EGFP) were routinely cultured in DMEM with high glucose supplemented with 10% fetal bovine serum in 80- or 175-cm^2 tissue culture flasks at 37°C in a 5% CO$_2$-humidified atmosphere. The HEK-GLP-1R cell line was generated using the Flp-In system (Invitrogen) by transfection of HEK-Flp-In cells with pcDNA5/FRT containing the hGLP-1R (NCBI database, accession NP_002053; Version, NP_002053.3; GI: 166795283) using Lipofectamine 2000 according to the manufacturer's instructions. Cells were then grown under selection using hygromycin B (400 U/ml), and clones were selected by dilution cloning and screened for expression of the GLP-1R on the basis of ^{125}I-GLP-1-(7-36) amide binding and functional coupling to the generation of cAMP (see below). To generate the GLP-1R-EGFP cDNA construct, the coding sequence of the full-length hGLP-1R containing Nhe1 and Xho1 restriction sites at the 5' and 3' ends, respectively, was cloned by polymerase chain reaction from the vector used for generation of the HEK-GLP-1R and ligated into the pEGFP-N1 vector. The construct contained an appropriately positioned Kozak sequence and start codon and used the stop codon of the EGFP-containing vector. The recombinant plasmid was purified and the sequence confirmed by automated sequence analysis (Protein Nucleic Acid Chemistry Laboratory, University of Leicester, Leicester, UK). After transfection using Lipofectamine 2000, a stable cell line was generated by selection with 1 mg/ml G418. Clones were isolated using cloning discs and after further growth, the expression of GLP-1R-EGFP was assessed by immunoblotting of EGFP using standard methods, visualization of EGFP fluorescence in live cells by confocal microscopy, and cAMP responses to GLP-1. The stable cell line was maintained in media containing 200 μg/ml G418.

Determination of Ligand Binding Affinity and Receptor Expression Levels

Membranes for binding experiments were prepared from confluent monolayers of cells in 80-cm^2 flasks. The cells were washed with 5 ml of 154 mM NaCl and 10 mM HEPES, pH 7.4, at 37°C, and detached using harvesting buffer (154 mM NaCl, 10 mM HEPES, and 5.4 mM EDTA, pH 7.4, at 37°C). Cells were collected by centrifugation (200g for 2 min at 4°C) and resuspended in 1 ml of homogenization buffer (10 mM HEPES and 10 mM EDTA, pH 7.4). Cells were then sonicated (Sonifier ultrasonic cell disruptor; Branson Ultrasonics Corporation, Danbury, CT) at 30% of the maximal amplitude for three times for 5 s each at ~30-s intervals and centrifuged (30,000g at 4°C for 10 min). The pellets were resuspended in resuspension buffer (10 mM HEPES and 0.1 mM EDTA, pH 7.4), protein concentration was adjusted to 2 mg/ml, and the samples were stored in aliquots at −80C until assay. Binding assays were carried out in round-bottomed 5-ml tubes in a total volume of 100 μl in binding buffer [Hanks' balanced salt solution containing 20 mM 0.1% (w/v) HEPES and bovine serum albumin (BSA), pH 7.4]. Reactions contained membrane (12.5 μg), ^{125}I-GLP-(7-36) amide (0.1 nM), and GLP-1-(7-36) amide at a range of concentrations (1 μM–1 pM). Binding was allowed to proceed to equilibrium by incubating at room temperature for 3 h. Membranes were then collected on Whatman GF/B glass fiber filters presoaked in 0.5% (v/v) polyethylenimine using a vacuum manifold (Millipore, Billerica, MA) washed through with 2% (w/v) BSA. Ice-cold wash buffer (2 ml; 25 mM HEPES, 1.5 mM CaCl$_2$, 1 mM MgSO$_4$, and 100 mM NaCl, pH 7.4) was added to the tube and the contents were immediately poured onto the membrane under vacuum. The tube was then washed with a further 2 ml

of wash buffer, which was added to the filter. Membranes were collected from tubes individually. After harvesting, filters were allowed to dry, and bound radioactivity was determined by gamma counter.

Determination of G Protein Activation

Determination of G protein activation was carried out by [^{35}S]GTPγS binding and immunoprecipitation of specific Gα subunits as described previously (Akam et al., 2001) using membranes prepared as described above. In brief, membranes (75 μg) were incubated with 1 μM (Gα$_s$ and Gα$_{q/11}$) or 10 μM (Gα$_{i/o/t/z/gust}$) GDP and 1 nM [^{35}S]GTPγS in assay buffer (10 mM HEPES, 100 mM NaCl, and 10 mM MgCl$_2$, pH 7.4). Where appropriate, tubes contained 10 μM GTPγS to determine nonspecific binding or GLP-1 as stated. After incubation for 5 min at 30°C (Gα$_s$) or 37°C (Gα$_{q/11}$ and Gα$_{i/o/t/z/gust}$), reactions were terminated with ice-cold assay buffer, and membranes were pelleted by centrifugation. Pellets were solubilized, precleared, and incubated overnight at 4°C with 5 μl of Gα subunit-specific antisera (1:100 dilutions). The resulting immune complexes were then isolated using protein A-Sepharose beads, collected by centrifugation, and washed repeatedly. Beads were then resuspended in scintillation fluid, and ^{35}S levels were determined.

Determination of cAMP

Intact Cells. Cells were grown to confluent monolayers in 24-well plates coated with 0.1% (w/v) poly-D-lysine and washed twice with 0.5 ml of Krebs-HEPES buffer (KHB; 10 mM HEPES, 4.2 mM NaHCO$_3$, 11.7 mM D-glucose, 1.18 mM MgSO$_4$·7H$_2$O, 1.18 mM KH$_2$PO$_4$, 4.69 mM KCl, 118 mM NaCl, and 1.3 mM CaCl$_2$·2H$_2$O, pH 7.4) containing 0.1% (w/v) BSA (KHB-BSA) before being incubated at 37°C for 10 min in KHB-BSA either with or without 500 μM isobutylmethylxanthine (IBMX) as indicated. Ligands (diluted in KHB-BSA) were added, and the reactions were terminated after the appropriate times by removal of the aqueous phase and addition of ice-cold 0.5 M trichloroacetic acid to allow subsequent determination of intracellular cAMP levels. When levels of cAMP in the extracellular buffer were also measured, the KHB-BSA was removed and placed in a 1.5-ml microcentrifuge tube containing an equal volume of ice-cold 1 M trichloroacetic acid.

Membranes. The generation of cAMP was determined based on a previously published method (Dimitriadis et al., 1991). After preparation of membranes exactly as described above, cAMP generation was determined in a total volume of 100 μl containing 10 mM HEPES, 12 mM MgCl$_2$, 60 mM NaCl, 1.2 mM EDTA, 1.2% BSA (w/v), 480 μM ATP, 1.2 mM IBMX, and 20 μg of membrane. Preparations were untreated (basal), stimulated with either forskolin (10 μM) or GTP (10 μM) or stimulated with either GLP-1-(7-36) amide (10 or 100 nM) or compound 2 (100 μM), both in the presence of GTP (10 μM). Where exendin-(9-39) was present, this was at either 100 nM or 1 μM. Reactions were initiated by addition of membranes. After incubation with slow agitation (5 min at 30°C), reactions were terminated by addition of an equal volume of ice-cold 1 M trichloroacetic acid.

In all cases, cAMP was extracted using a method identical to that for the extraction of inositol 1,4,5-trisphosphate (Willars and Nahorski, 1995), and levels were determined by a competitive radioreceptor assay using binding protein purified from bovine adrenal glands (Brown et al., 1971) and related to cellular protein levels that were determined by Bradford assay (Bradford, 1976).

Determination of Changes in the Intracellular Ca^{2+} Concentration

For determination of changes in intracellular Ca^{2+} concentration ([Ca^{2+}]$_i$) in cell populations, cells were grown to approximately 90% confluence in 96-well plates coated with 0.1% (w/v) poly-D-lysine and loaded with 2 μM fluo-4-AM diluted in KHB-BSA containing 0.036%

(w/v) Pluronic acid for 40 min at room temperature. Monolayers were then washed, equilibrated for 10 min, and fluorescence was recorded at 37°C in KHB-BSA as an index of [Ca^{2+}]$_i$ using a microplate reader (NOVOstar; BMG Labtech, Aylesbury, UK) as described previously (Heding et al., 2002). For intracellular Ca^{2+} imaging, cells were plated into six-well plates (approximately 0.5 × 10^6 cells/well) containing 25-mm-diameter glass coverslips precoated with 0.1% (w/v) poly-D-lysine and allowed to adhere for 24 to 48 h. Cells were then loaded with fluo-4-AM as described above and mounted in a perfusion chamber containing KHB heated to 37°C with a Peltier unit. The chamber volume was 0.5 ml and where required was perfused at 5 ml/min. Cells were imaged using an UltraVIEW confocal microscope (PerkinElmer Life and Analytical Sciences), with a 40× oil immersion objective lens and a 488 nm krypton/argon laser line. Emitted light was collected above 510 nm, and images captured at a rate of approximately 1 frame/s using a charge-coupled device camera. Data analysis was carried out using the Imaging Suite (PerkinElmer Life and Analytical Sciences), with raw cytosolic fluorescence data exported to Excel (Microsoft, Redmond, WA) and expressed as fluorescence/basal fluorescence for each cell.

Live-Cell Imaging of EGFP-Tagged GLP-1Rs and Determination of Internalization

HEK-GLP-1R-EGFP cells were grown on coverslips, rinsed with KHB, and mounted in a perfusion chamber containing KHB at 37°C as described above. Cells were then imaged using an UltraVIEW confocal microscope as described above. Ligand was added directly to the chamber in 200 μl of prewarmed KHB. Vehicle controls were used as appropriate. Images were captured at 0, 2.5, 5, 10, 20, 30, 40, 50, and 60 min. For at least six individual cells on each coverslip and with at least three coverslips per experimental condition, fluorescence intensity was measured at a region of the plasma membrane and within the cytosolic compartment, and a measure of internalization derived using the equation $1 - (Fm_t/Fc_t)/(Fm_b/Fc_b)$, where Fm_t and Fc_t represent the fluorescence intensity (in arbitrary units) at time t at the plasma membrane and in the cytosol, respectively, and Fm_b and Fc_b represent these parameters under basal conditions at the start of the experiment.

Assessment of Cell Viability by Trypan Blue Exclusion

Cells were grown as monolayers in 24-well plates coated with 0.1% (w/v) poly-D-lysine and washed twice with KHB-BSA before being incubated at 37°C for 10 min in KHB-BSA containing 500 μM IBMX. Ligands in KHB-BSA were added for 90 min at 37°C before being aspirated and 500 μl of 0.02% (w/v) trypan blue in KHB added. Cells were viewed using an ECLIPSE TE2000 inverted microscope (Nikon Instruments Europe, Badhoevedorp, The Netherlands) with a 40× objective, and bright field images were captured using a Digital Sight camera (Nikon Instruments Europe) and associated software (Nikon Instruments Europe). Cells excluding trypan blue after 5 to 10 min were regarded as viable, whereas those in which the cytoplasm was blue were regarded as nonviable.

Data Analysis

The K_d and B_{max} values were determined using standard analysis of homologous competition binding data using Prism version 5.00 for Windows (GraphPad Software Inc., San Diego, CA). Concentration-response curves were also fitted using Prism, according to a standard four-parameter logistic equation. Where the data were best described by a bell-shaped curve, the data were fitted using the appropriate equation in Prism, with nH1 and nH2 constrained to 1. The apparent pA_2 value of exendin-(9-39) was calculated based on the equation log (DR−1) − log [antagonist], where DR is the dose ratio (Kenakin, 2004). All data are presented as mean +/− S.E.M., where $n = 3$ unless otherwise stated.

Results

Signaling Mediated by GLP-1-(7-36) Amide in HEK-GLP-1R Cells. HEK-Flp-In cells with stable expression of the hGLP-1R (HEK-GLP-1R cells) were initially characterized by examining the binding and signaling of GLP-1-(7-36) amide. Homologous competition binding revealed a K_d value for GLP-1-(7-36) amide of -8.95 ± 0.09 log$_{10}$ M and a B_{max} value of 1061 ± 223 fmol/mg protein. G protein activation by GLP-1-(7-36) amide in membranes prepared from HEK-GLP-1R cells was assessed by specific Gα immunoprecipitation and determination of bound [^{35}S]GTPγS following agonist challenge. Under these circumstances, using a concentration of GLP-1-(7-36) amide that was maximal for both cAMP and intracellular Ca^{2+} responses (30 nM; see below), an increased association of ^{35}S was observed with Gα_s but not with G$\alpha_{i/o}$ or G$\alpha_{q/11}$ (Fig. 1a). The ability of the G$\alpha_{i/o}$ and G$\alpha_{q/11}$ antibodies to immunoprecipitate the relevant activated G proteins was confirmed using membranes prepared from Chinese hamster ovary cell lines recombinantly expressing either G$\alpha_{i/o}$-coupled muscarinic M$_2$ receptors or G$\alpha_{q/11}$-coupled muscarinic M$_3$ receptors (Burford et al., 1995) challenged with the muscarinic receptor agonist methacholine (1 mM; data not shown).

GLP-1-(7-36) amide stimulated a time-dependent, robust increase in cAMP production in intact HEK-GLP-1R cells, which in the absence of the phosphodiesterase inhibitor IBMX reached a maximum after approximately 15 min (Fig. 1b). The increase in cAMP was also concentration-dependent, with a pEC$_{50}$ value at 10 min of 10.07 ± 0.14 (85 pM; Fig. 1c). Pretreatment of cells for 10 min with the GLP-1R antagonist exendin-(9-39) (100 nM), and its continued presence during stimulation with GLP-1-(7-36) amide resulted in a dextral shift of the concentration-response curve (Fig. 1c), with an apparent pA$_2$ value for exendin-(9-39) of 7.29 ± 0.07 (52 nM). Pretreatment of cells with exendin-(9-39) for 60 min did not significantly alter the apparent pA$_2$ value (7.33 ± 0.16, 47 nM; graphs not shown). Although CTX activates Gα_s, extended treatment can down-regulate Gα_s and can therefore, in some circumstances, be used to assess involvement in cellular responses (Seidel et al., 1999). Here, 24-h treatment of HEK-GLP-1R cells with CTX reduced cAMP generation in response to a maximal concentration of GLP-1-(7-36) amide (Fig. 1d). However, CTX treatment markedly elevated "basal" levels of cAMP in the absence of ligand and had no effect on cAMP generation by a lower concentration (0.1 nM) of GLP-1-(7-36) amide (Fig. 1d).
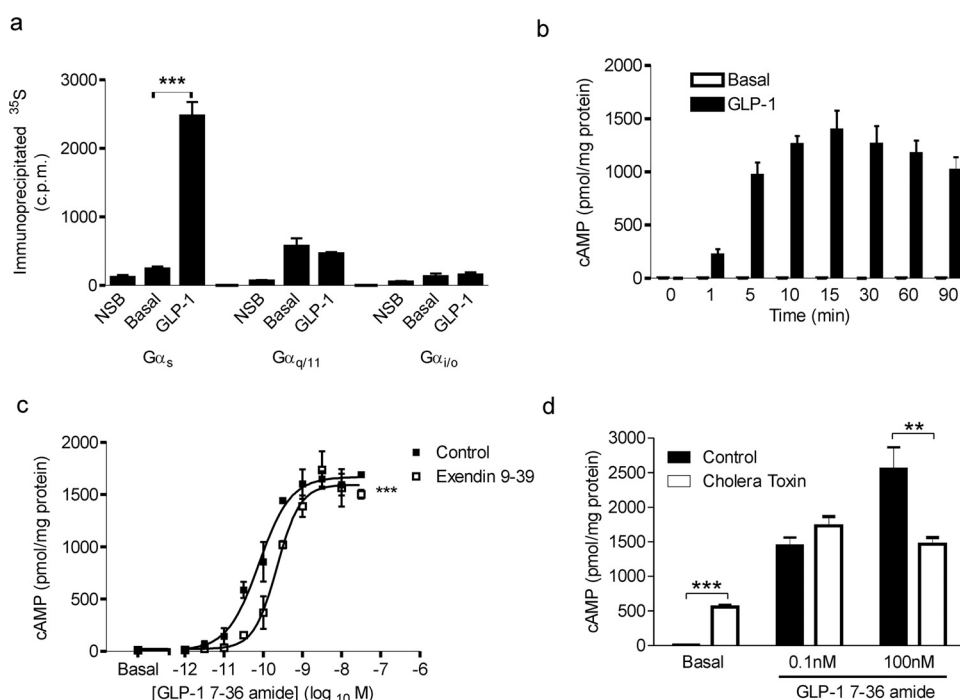
Fig. 1. GLP-1 couples the GLP-1R to Gα_s proteins and induces cAMP generation in HEK-GLP-1R cells. a, membranes from HEK-GLP-1R cells were incubated in the presence of 1 μM (Gα_s and G$\alpha_{q/11}$) or 10 μM (G$\alpha_{i/o}$) GDP and 1 nM [^{35}S]GTPγS and then either treated with vehicle (KHB; basal) or challenged with 30 nM GLP-1-(7-36) amide for 5 min. Nonspecific binding (NSB) was determined in the presence of 10 μM GTPγS. Immunoprecipitation was carried out using antibodies against specific Gα subunits as indicated, and associated ^{35}S levels were determined. ***, $p < 0.001$ (by Bonferroni's test after one-way analysis of variance; for clarity, only GLP-1 versus basal comparisons are shown). b, HEK-GLP-1R cells were treated for the indicated times up to 90 min with either 30 nM GLP-1-(7-36) amide or vehicle (KHB; basal) in the absence of IBMX and intracellular levels of cAMP determined and expressed relative to cellular protein content. c, HEK-GLP-1R cells were pretreated for 10 min with either the GLP-1R antagonist exendin-(9-39) (100 nM) or vehicle (KHB; basal) in the presence of IBMX (500 μM) before being challenged for 10 min with the indicated concentrations of GLP-1-(7-36) amide. Intracellular levels of cAMP were determined and expressed relative to cellular protein content. In the absence and presence of exendin-(9-39), respectively, the pEC$_{50}$ values were 10.07 ± 0.14 and 9.60 ± 0.10, the E_{max} values were 1619 ± 90 and 1549 ± 124 pmol/mg protein, and the Hill slope values (n_H) were 1.19 ± 0.10 and 1.63 ± 0.31. ***, $p < 0.001$ for control curves versus exendin-(9-39) pretreated curves (by two-way analysis of variance). d, HEK-GLP-1R cells were either pretreated with vehicle (control) or 2 μg/ml cholera toxin for 24 h. In the presence of IBMX (500 μM), they were then either treated with vehicle (KHB; basal) or challenged with GLP-1-(7-36) amide (0.1 or 100 nM) for 10 min, and levels of intracellular cAMP were determined relative to cellular protein content. **, $p < 0.01$ by Student's t test. All data are mean $+/\pm$ S.E.M., $n \geq 3$.

In fluo-4-loaded populations of HEK-GLP-1R cells, GLP-1-(7-36) amide evoked a rapid increase in fluorescence (reflecting an increase in $[Ca^{2+}]_i$), which was followed by a slower decline (Fig. 2a). The maximal response after addition of GLP-1-(7-36) amide was concentration-dependent (Fig. 2, a and b), with a pEC_{50} value of 10.18 ± 0.16 (67 pM). In the presence of 100 nM exendin-(9-39), the pEC_{50} value was relatively unaffected (10.18 ± 0.16 in control versus 9.79 ± 0.11 in the presence of exendin-(9-39)), but the curve was partially collapsed (E_{max} reduced to $79 \pm 3\%$ of control; Fig. 2b). The Ca^{2+} response to GLP-1-(7-36) amide was unaffected by removal of extracellular Ca^{2+} but

was almost abolished by pretreatment with the sarco/endoplasmic reticular Ca^{2+}-ATPase inhibitor thapsigargin to deplete intracellular Ca^{2+} stores (Fig. 2c). Pretreatment of cells with either the putative inhibitor of phospholipase C U73122, its aminosteroid negative control U73343, or overnight treatment with pertussis toxin to ADP-ribosylate and inactivate $G\alpha_{i/o}$ proteins had no effect on the Ca^{2+} responses to GLP-1-(7-36) amide (Fig. 2d). Experiments with U73122 and U73343 were performed in nominally Ca^{2+}-free buffer to avoid potential effects of these compounds on Ca^{2+} entry across the plasma membrane (Werry et al., 2003). Single-cell confocal imaging of
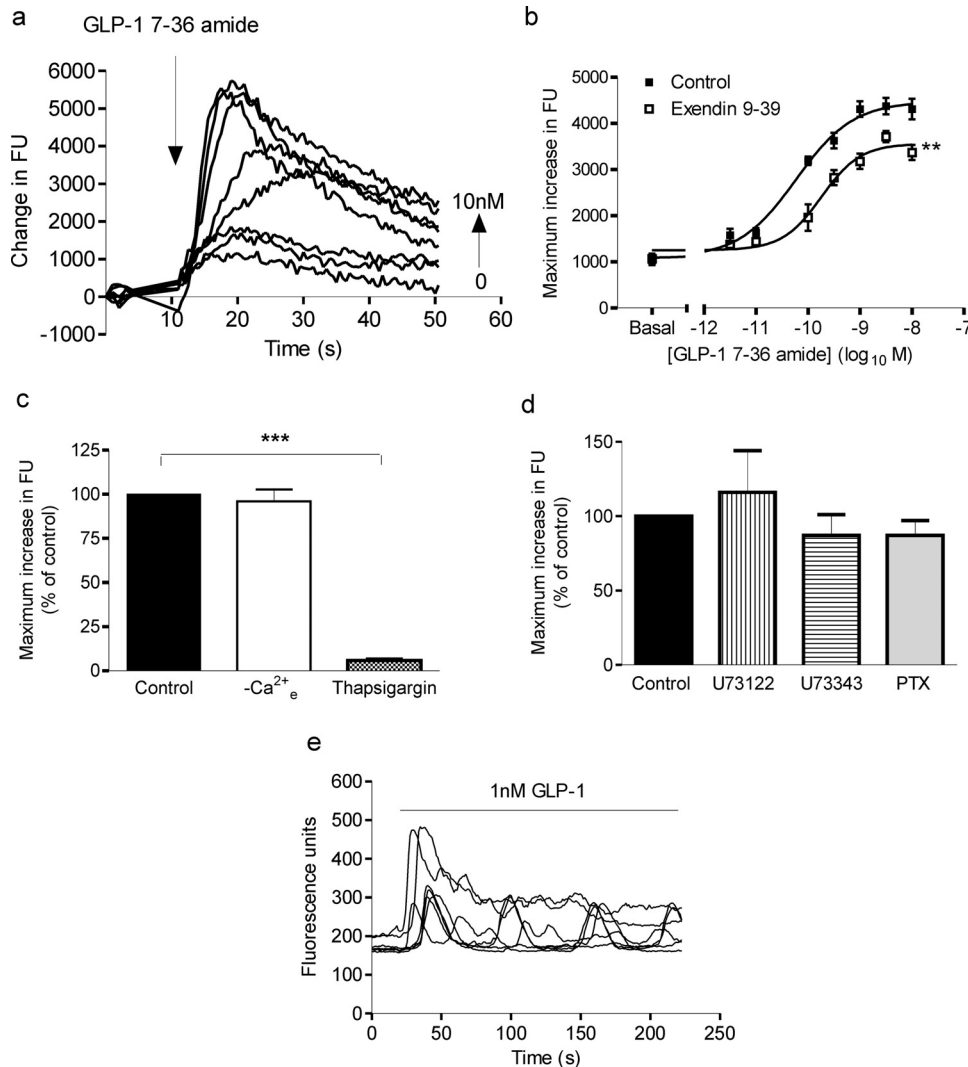

Fig. 2. GLP-1-mediated Ca^{2+} responses in HEK-GLP-1R cells. HEK-GLP-1R cells were grown in 96-well plates and loaded with the calcium indicator fluo-4. Cells were then challenged with GLP-1-(7-36) amide or KHB (0), and changes in fluorescence were recorded using a microplate reader as an index of changes in $[Ca^{2+}]_i$. a, representative family of traces induced by GLP-1-(7-36) amide, which was added at the time indicated by the arrow at 0 to 10 nM. b, cells were pretreated for 1 h with either 100 nM exendin-(9-39) or KHB (control) and then challenged with either vehicle (KHB; basal) or the indicated concentrations of GLP-1-(7-36) amide. The maximal change in fluorescence units (FU) was determined in each instance to allow generation of concentration-response curves. The pEC_{50} values were 10.18 ± 0.16 for GLP-1-(7-36) amide alone and 9.79 ± 0.11 in the presence of exendin-(9-39). All data are mean $\pm$ S.E.M., $n = 3$. **, $p < 0.01$ for control curves versus exendin-(9-39) pretreated curves (by two-way analysis of variance). c, cells were either treated as normal (control), washed, and treated in KHB without Ca^{2+} ($-Ca^{2+}_e$) or pretreated with 2 μM thapsigargin for 5 min. Maximal responses after addition of 10 nM GLP-1-(7-36) amide were then recorded and are expressed relative to control samples. Data are mean + S.E.M., $n = 3$ to 4. ***, $p < 0.001$ (by Bonferroni's test after one-way analysis of variance, with statistical analysis performed on the raw data). d, cells were pretreated with either the putative inhibitor of phospholipase C U73122 or its aminosteroid negative control U73343 (both 30-min pretreatment; 10 μM) or alternatively treated for 20 h with pertussis toxin (PTX; 100 ng/ml). Maximal responses after addition of 100 nM GLP-1-(7-36) amide were then recorded and expressed relative to control samples. Stimulations with GLP-1-(7-36) amide in the presence of either U73122 or U73343 were performed in the absence of extracellular Ca^{2+}. Data are mean + S.E.M., $n = 3$ to 6. e, cells were grown on glass coverslips, loaded with fluo-4, and imaged by confocal microscopy. Cells were then challenged with 1 nM GLP-1-(7-36) amide. Traces are representative of at least four independent experiments.
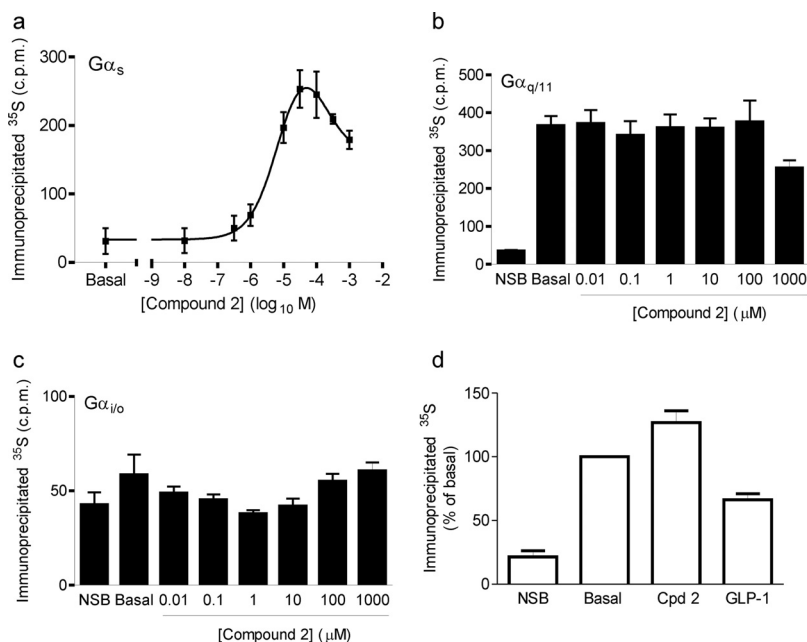
Fig. 3. Compound 2 couples the GLP-1R to $G\alpha_s$ but not $G\alpha_{q/11}$ or $G\alpha_{i/o}$ proteins. Membranes from HEK-GLP-1R or HEK-Flp-In cells were incubated in the presence of 1 μM ($G\alpha_s$ and $G\alpha_{q/11}$) or 10 μM ($G\alpha_{i/o}$) GDP and 1 nM [^{35}S]GTPγS and then challenged with agonist or vehicle [5% (v/v) DMSO; basal] where appropriate for 5 min. Non-specific binding (NSB) was determined using 10 μM GTPγS (and subtracted from values in a). Immunoprecipitation was carried out using antibodies against specific $G\alpha$ subunits as indicated, and associated ^{35}S levels were determined. a to c, membranes from HEK-GLP-1R cells were stimulated with the indicated concentrations of compound 2 and a $G\alpha_s$- (a), $G\alpha_{q/11}$- (b), or $G\alpha_{i/o}$ (c)-specific antibody was used for immunoprecipitation. The pEC_{50} value for the rising phase in a was 5.36 $\pm$ 0.16 (4.4 μM). Using the $G\alpha_s$ antibody, the response to 30 nM GLP-1 was 1506 $\pm$ 128 cpm (with NSB subtracted), whereas the maximal response to compound 2 was 245 $\pm$ 32 cpm. d, membranes from HEK-Flp-In cells were stimulated with either vehicle (basal), compound 2 (10 μM), or GLP-1-(7-36) amide (30 nM) and a $G\alpha_s$-specific antibody was used for immunoprecipitation. Data are mean $\pm$ or $+$ S.E.M., $n = 3$ to 4.

fluo-4-loaded HEK-GLP-1R cells demonstrated that GLP-1-(7-36) amide increased fluorescence in all cells and particularly at submaximal concentrations was sometimes associated with oscillatory changes in $[Ca^{2+}]_i$ (Fig. 2e; data not shown).

Signaling Mediated by Compound 2 in HEK-GLP-1R Cells. Challenge of membranes prepared from HEK-GLP-1R cells with compound 2 in the presence of [^{35}S]GTPγS resulted in a concentration-dependent increase in the association of ^{35}S with $G\alpha_s$ (Fig. 3a). However, the concentration-response curve was bell-shaped, with the response reaching a maximum at 10 μM and declining thereafter. The pEC_{50} value of the rising phase of this curve was 5.36 $\pm$ 0.16 (4.4 μM; $n = 4$), with a maximal response of 16 $\pm$ 2% of the response to 30 nM GLP-1-(7-36) amide. Compound 2 had no effect on the asso-

ciation of ^{35}S with either $G\alpha_{q/11}$ or $G\alpha_{i/o}$ (Fig. 3, b and c). Neither compound 2 nor GLP-1-(7-36) amide stimulated an increase in the association of ^{35}S with $G\alpha_s$ in membranes prepared from HEK-Flp-In cells (Fig. 3d) or wild-type HEK-293 cells (data not shown).

Challenge of HEK-GLP-1R cells for 10 min with compound 2 resulted in a concentration-dependent increase in intracellular cAMP levels (Fig. 4a), with a pEC_{50} value of 6.23 $\pm$ 0.07 (0.59 μM). The maximal cAMP production in response to compound 2 was 88 $\pm$ 8% of that produced by a maximal concentration of GLP-1 (30 nM). Neither compound 2 nor GLP-1-(7-36) amide stimulated an increase in cAMP in HEK-Flp-In cells (Fig. 4b) or wild-type HEK-293 cells (data not shown). The response to a submaximal (1 μM) concentration of compound 2 was time-dependent, showing an increase in
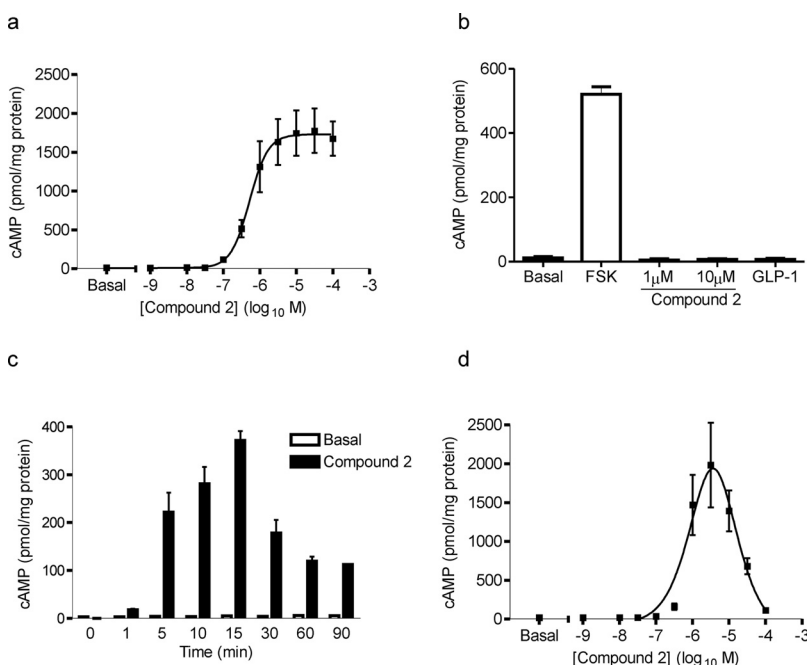

Fig. 4. Compound 2 induces cAMP generation in HEK-GLP-1R cells. HEK-GLP-1R or HEK-Flp-In cells were challenged with either vehicle (basal), forskolin, compound 2, or GLP-1-(7-36) amide in the presence of IBMX (500 μM) unless otherwise stated. Levels of intracellular cAMP were determined relative to the cellular protein content. The final concentration of DMSO (vehicle) was 5% (v/v) in all cases. a, HEK-GLP-1R cells were treated with vehicle (basal) or the indicated concentrations of compound 2 for 10 min; the pEC_{50} was 6.23 $\pm$ 0.07. The response to 30 nM GLP-1 in parallel experiments was 2017 $\pm$ 371 pmol cAMP/mg protein. Data are mean $\pm$ S.E.M., $n = 3$. b, HEK-Flp-In cells were treated for 10 min with vehicle (basal), forskolin (FSK; 10 μM), compound 2 (1 or 10 μM), or GLP-1-(7-36) amide (30 nM). Data are mean $+$ S.E.M., $n = 3$. c, HEK-GLP-1R cells were treated for up to 90 min with 1 μM compound 2 or vehicle (basal) but in the absence of IBMX. Data are mean $+$S.D. from duplicates within one experiment, representative of two other experiments. d, HEK-GLP-1R cells were treated with vehicle (basal) or the indicated concentrations of compound 2 for 90 min. Data are mean $\pm$ S.E.M., $n = 4$.

levels up to approximately 15 min but a subsequent rapid decline in the absence of IBMX (Fig. 4c). In contrast to the original study on compound 2 that reported a bell-shaped concentration-response curve (Knudsen et al., 2007), the curve shown here was clearly sigmoidal. However, our assay was much shorter and when the assay was extended to 90 min in line with the original study, the concentration dependence of compound 2-mediated cAMP responses showed a very pronounced bell-shaped relationship, which reached a maximum at approximately 3 μM and a dramatic decline at higher concentrations (Fig. 4d). The potency of compound 2 for this response was approximated by fitting a truncated curve with concentrations between 0.001 and 3 μM. This gave a pEC_{50} value of 6.18 $\pm$ 0.05 (0.66 μM; $n = 4$), which was not significantly different from the value determined at 10 min. Stimulating cells for 90 min with GLP-1-(7-36) amide did not result in a bell-shaped concentration-response curve. The curve was sigmoidal, with a pEC_{50} value of 9.94 $\pm$ 0.09

(graph not shown), which was not significantly different from that at 10 min (10.07 $\pm$ 0.14).

In the experiments measuring cAMP described above, the extracellular buffer was removed before terminating the reaction to allow the measurement of intracellular cAMP levels. To assess whether the downward slope of the bell-shaped concentration-response curve to compound 2 at 90 min of stimulation was a consequence of reduced cAMP generation or reduced cellular retention, we measured both intracellular and extracellular levels of cAMP. Exposure of HEK-GLP-1R cells to either forskolin, approximately EC_{50} (100 pM) or high (30 nM) concentrations of GLP-1-(7-36) amide or an approximate EC_{50} concentration of compound 2 (1 μM) resulted in similar proportions of extracellular and intracellular cAMP (Fig. 5a). In contrast, cAMP measured in response to challenge with a high (100 μM) concentration of compound 2 was predominantly extracellular and, as expected from the bell-shaped concentration-response curve, considerably lower
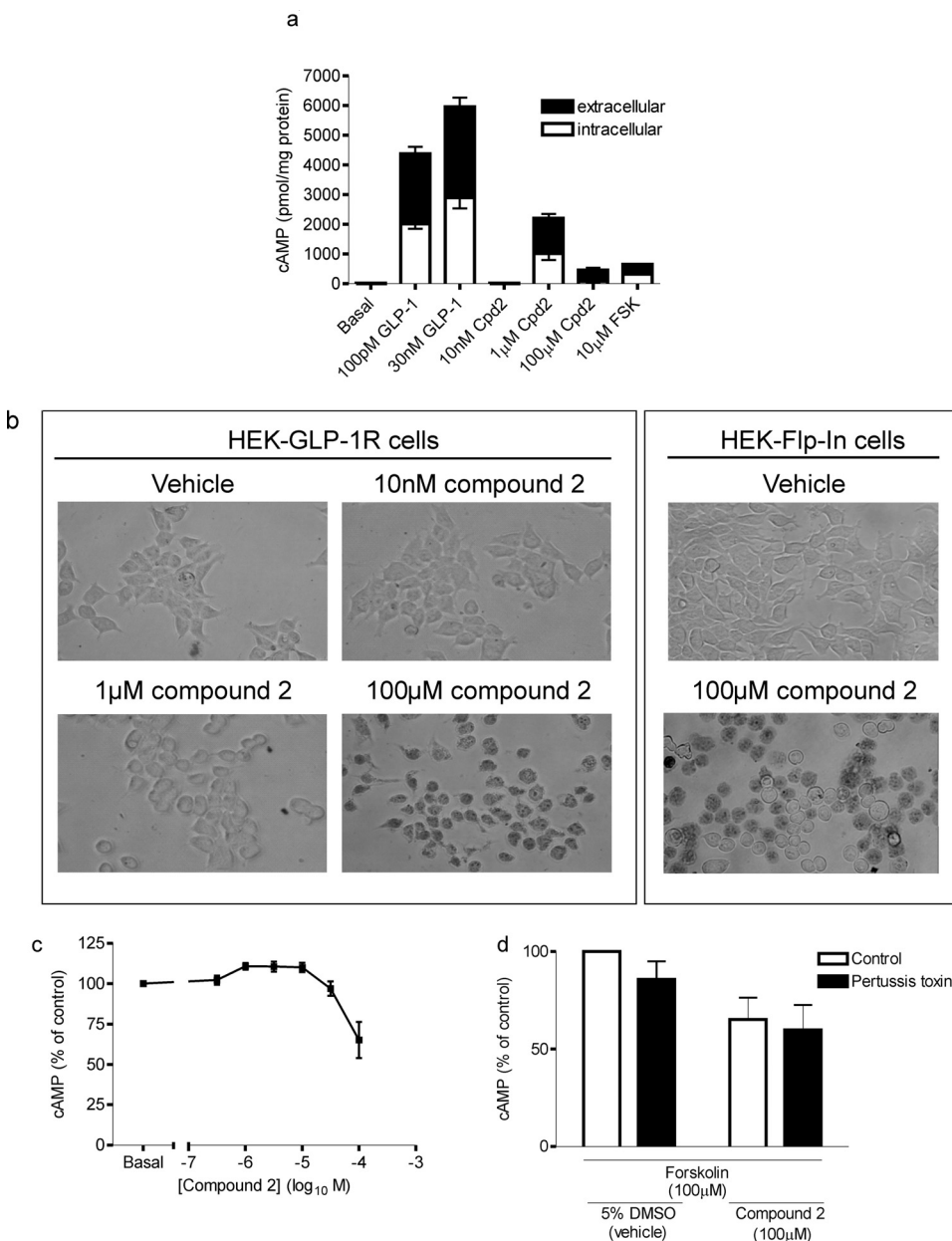

Fig. 5. Cytotoxic effects of compound 2. a, HEK-GLP-1R cells were treated for 90 min with vehicle [5% (v/v) DMSO; basal], GLP-1-(7-36) amide, compound 2 (Cpd2), or forskolin (FSK), and both intracellular and extracellular cAMP were measured separately as described under *Materials and Methods*. Data are mean + or − S.E.M., $n = 3$. b, HEK-GLP-1R or control (not transfected with the GLP-1R) HEK-Flp-In cells were treated with vehicle [5% (v/v) DMSO] or compound 2 at the indicated concentrations in the presence of IBMX (500 μM) for 90 min, washed, and stained with 0.02% trypan blue. Cells were viewed with a 40× objective lens. Data are representative images of three separate experiments where each treatment was carried out in duplicate. c, HEK-GLP-1R cells were treated with forskolin (100 μM), and the indicated concentrations of compound 2 for 90 min in the presence of IBMX (500 μM) and 5% (v/v) DMSO (vehicle), and levels of intracellular cAMP were determined relative to cellular protein content. d, cells were cultured in the absence (control) or presence of pertussis toxin (100 ng/ml) for ~20 h and then stimulated with forskolin (100 μM) in the presence of either vehicle [5% (v/v) DMSO] or compound 2 (100 μM) as in c. Data in c and d are mean $\pm$ or + S.E.M., $n = 3$ to 4.

than levels generated by the lower concentration of compound 2 (Fig. 5a). After 90 min of challenge with high concentrations of compound 2, cells lost their flattened morphology and rounded up. Thus, cellular morphology was assessed along with a determination of viability using trypan blue exclusion. Treatment of cells with vehicle [5% (v/v) DMSO] or a low concentration of compound 2 (10 nM) did not affect cell morphology or viability (Fig. 5b). At an approximately EC_{50} concentration of compound 2 (1 μM), the cells had a much more rounded morphology but remained viable as judged by their ability to exclude trypan blue. At higher concentrations of compound 2 (e.g., 100 μM; Fig. 5b), in addition to rounding up, cells were no longer able to exclude trypan blue, indicating a loss of viability. These higher concentrations of compound 2 had similar effects on HEK-Flp-In cells (Fig. 5b) and wild-type HEK-293 cells not expressing the GLP-1R (data not shown). Concentrations of compound 2 greater than 10 μM also inhibited forskolin-stimulated cAMP accumulation (Fig. 5c). Overnight treatment of HEK-GLP-1R cells with pertussis toxin did not influence forskolin-stimulated cAMP generation and did not influence the inhibitory effect of a high concentration of compound 2 (100 μM) on this forskolin-stimulated cAMP generation (Fig. 5d).

The cAMP response to a maximal concentration of compound 2 (10 μM) was only partially attenuated by CTX treatment (Fig. 6a). In addition, the cAMP response to an approximately EC_{50} concentration of compound 2 (1 μM) was unaffected by CTX treatment (Fig. 6a). These effects of CTX that were dependent on agonist concentration were clearly shown when full concentration-response curves for compound 2-mediated cAMP generation in the absence and presence of pretreatment with CTX were constructed (Fig. 6b). These experiments again showed that CTX caused an increase in basal levels of cAMP (Fig. 6, a and b).

In contrast to the dextral shift of the cAMP concentration-response curve for GLP-1-(7-36) amide by pretreatment with 100 nM exendin-(9-39) (Fig. 1c), this orthosteric antagonist did not cause a similar shift in the concentration-response curve for compound 2-mediated cAMP generation. The presence of exendin-(9-39) did, however, increase the E_{max} value of compound 2 to 137 $\pm$ 17% of control ($n = 4$) without a significant effect on the pEC_{50} value (6.02 $\pm$ 0.07 for control versus 6.17 $\pm$ 0.09 with exendin-(9-39); $n = 4$; Fig. 7a). At progressively higher concentrations of exendin-(9-39) (up to 3 μM), the antagonist caused significant reductions in the cAMP response to an approximate EC_{50} concentration of GLP-1-(7-36) amide (100 pM). However, these increasing concentrations of exendin-(9-39) only enhanced the magnitude of the response to an approximately EC_{50} concentration of compound 2 (1 μM; Fig. 7b). To investigate potential in-

teractions between compound 2 and GLP-1-(7-36) in our cell line, similar experiments were performed to those described in the original identification of compound 2 (Knudsen et al., 2007). Thus, HEK-GLP-1R cells were costimulated for 10 min and changes in intracellular cAMP levels were assessed. As also shown above, compound 2 acted as an agonist and caused a concentration-dependent increase in cAMP levels in the absence of GLP-1-(7-36) amide (Fig. 7c; control). The E_{max} value of the response to GLP-1-(7-36) amide was identical in the presence and absence of compound 2. Costimulation of the cells with 10 nM GLP-1-(7-36) amide and 100 μM forskolin resulted in a response that was 22 $\pm$ 3% greater than GLP-1-(7-36) amide alone (data not shown), indicating that the lack of additivity at E_{max} values was not through an inability to detect further increases. Although the E_{max} value was unaffected, the potency of GLP-1-(7-36) amide was significantly reduced with increasing concentrations of compound 2 ($p < 0.05$; F-test).

Addition of compound 2 to populations of fluo-4-loaded cells caused an initial rapid increase in the fluorescence signal that was a consequence of the fluorescent properties of the compound (Fig. 8a) because this increase was apparent on the addition to buffer in the absence of cells and fluo-4 (data not shown). Compound 2 evoked a concentration-dependent, slowly rising increase in $[Ca^{2+}]_i$ that was longer lasting than that in response to GLP-1-(7-36) amide (Fig. 8, a and b). The time to the maximal change in fluorescence was greater after addition of compound 2 (100 μM; 36.4 $\pm$ 10.0 s; $n = 4$) than after GLP-1-(7-36) amide (100 nM; 21.6 $\pm$ 1.5 s; $n = 4$). We were unable to determine the potency of compound 2 for this response as solubility and toxicity issues with DMSO limited the use of higher concentrations. The initial rapid increase in fluorescence on addition of compound 2 (100 μM) was present in HEK-Flp-In cells (Fig. 8c). Compound 2 also caused a small gradual increase in fluorescence in these HEK-Flp-In cells (Fig. 8c) and wild-type HEK-293 cells (data not shown), but this was distinguishable from responses in cells expressing the GLP-1R (Fig. 8a). The maximal Ca^{2+} response to 100 μM compound 2 was abolished by pretreatment of cells with thapsigargin (2 μM; 5 min; Fig. 8d) but unaffected by removal of extracellular Ca^{2+} (Fig. 8d). Pretreatment of cells with either U73122 or U73343 (and subsequent challenge with compound 2 in the absence of extracellular Ca^{2+}) or alternatively overnight treatment with pertussis toxin had no effect on the Ca^{2+} responses to compound 2 (Fig. 8e). Exendin-(9-39) (100 nM; 10-min pretreatment) had no significant effect on the maximal $[Ca^{2+}]_i$ change in response to 100 μM compound 2 (60.8 $\pm$ 5.6 and 71.3 $\pm$ 2.7% of the response to 100 nM GLP-1-(7-36) amide in the absence and presence of exendin-(9-39), respectively).
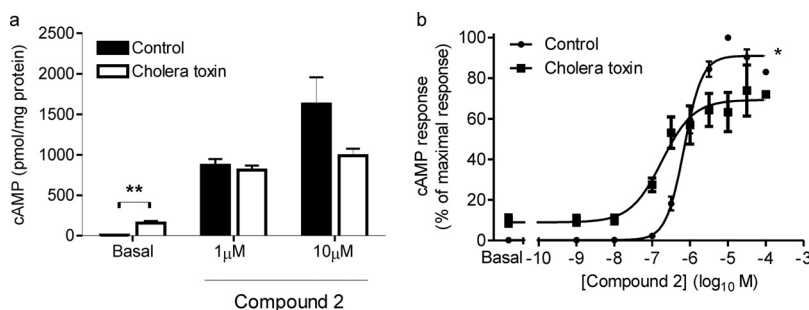
Fig. 6. Cholera toxin sensitivity of GLP-1R-mediated cAMP generation by compound 2. HEK-GLP-1R cells were either pretreated with vehicle (control) or 2 μg/ml cholera toxin for ~20 h. Cells were then either challenged with vehicle [5% (v/v) DMSO; basal] or compound 2 as indicated in the presence of IBMX (500 μM) for 10 min, and the levels of intracellular cAMP were determined relative to cellular protein content. Data are mean + or $\pm$ S.E.M., $n = 5$ (a) or 3 (b). **, $p < 0.01$ by Student's paired t test (a); *, $p < 0.05$ by two-way analysis of variance (b); pEC_{50} values of 6.10 $\pm$ 0.07 (control) and 6.73 $\pm$ 0.03 (cholera toxin), $p < 0.05$ by Student's paired t test.
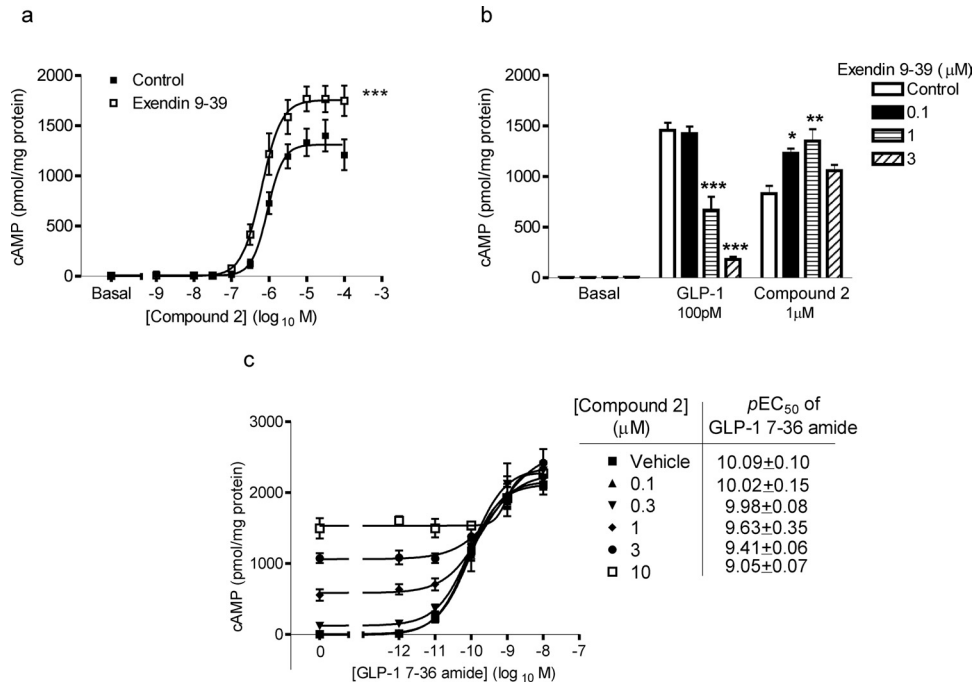
Fig. 7. Functional interaction of compound 2 with exendin-(9-39) and GLP-1-(7-36) amide. HEK-GLP-1R cells were treated with vehicle [5% (v/v) DMSO; basal], compound 2, or GLP-1-(7-36) amide in the presence of IBMX (500 μM), and levels of intracellular cAMP were determined relative to cellular protein content. a, cells were pretreated for 10 min with either exendin-(9-39) (100 nM) or KHB (control) and then stimulated with the indicated concentrations of compound 2 for 10 min. ***, $p < 0.001$ versus control by two-way analysis of variance. b, cells were pretreated for 10 min with exendin-(9-39) (0.1–3 μM) or KHB (control) and then challenged with vehicle [5% (v/v) DMSO] submaximal concentrations of either GLP-1-(7-36) amide (100 pM) or compound 2 (1 μM) for 10 min. *, $p < 0.05$; **, $p < 0.01$; and ***, $p < 0.001$ compared with control by Dunnett's test after one-way analysis of variance. c, cells were treated for 10 min with either vehicle [5% (v/v) DMSO] or compound 2 at the indicated concentrations and either buffer (KHB; 0) or GLP-1-(7-36) amide at the concentrations indicated on the abscissa. The pEC_{50} values for GLP-1-(7-36) amide-mediated cAMP generation in the presence of the different concentrations of compound 2 are given in the table; $p < 0.05$ for these values by F-test. All data are mean ± or + S.E.M., $n = 3$ to 4.
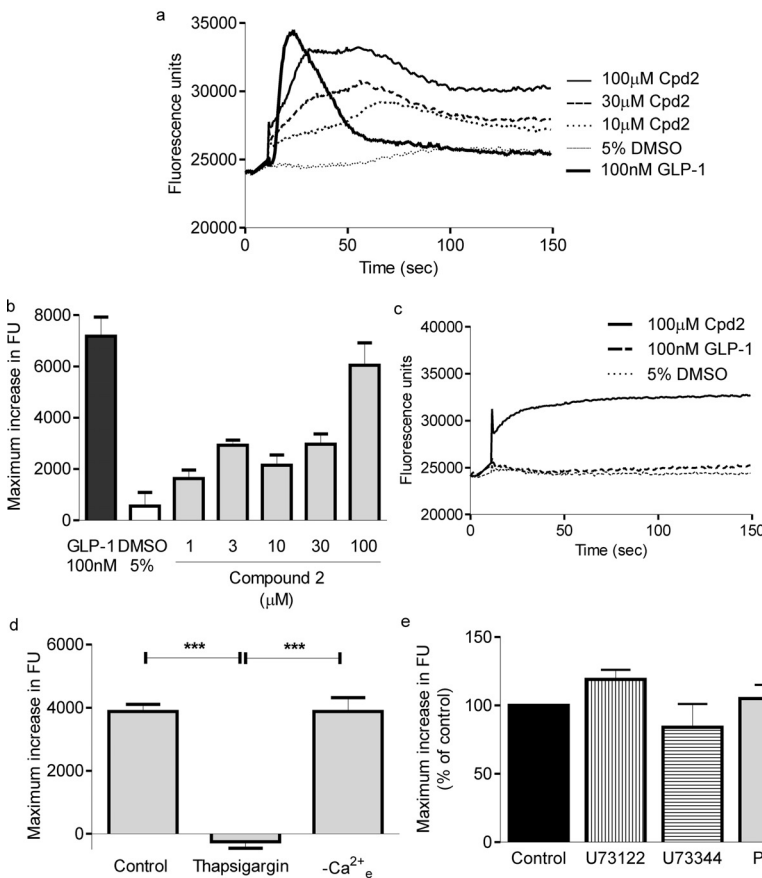

Fig. 8. Compound 2-mediated Ca^{2+} signaling. Cells were grown in 96-well plates and loaded with the Ca^{2+} indicator fluo-4. Cells were then challenged with either vehicle [5% (v/v) DMSO], compound 2, or GLP-1-(7-36) amide as indicated and changes in fluorescence recorded using a microplate reader as an index of changes in $[Ca^{2+}]_i$. a, representative traces showing Ca^{2+} responses in HEK-GLP-1R cells. b, maximal Ca^{2+} responses to the indicated concentrations of compound 2, vehicle [5% (v/v) DMSO] or GLP-1-(7-36) amide in HEK-GLP-1R cells. c, representative traces after addition of GLP-1-(7-36) amide, compound 2, or vehicle to HEK-Flp-In cells. d, HEK-GLP-1R cells were either treated as normal (control), washed, and treated in KHB without Ca^{2+} ($-Ca^{2+}_e$), or pretreated with 2 μM thapsigargin for 5 min. Maximal responses after addition of 100 μM compound 2 were then determined. Traces are either representative of $n =$ 3 to 4 or mean + S.E.M. ***, $p < 0.001$ (by Bonferroni's test after one-way analysis of variance). e, HEK-GLP-1R cells were pretreated with either U73122 or U73343 (30-min pretreatment; 10 μM) or alternatively treated for 20 h with pertussis toxin (PTX; 100 ng/ml). Maximal responses after addition of 30 μM compound 2 were then recorded and are expressed relative to control samples. Stimulations with compound 2 in the presence of either U73122 or U73343 were performed in the absence of extracellular Ca^{2+}. Data are mean + S.E.M., $n = 3$ to 5.
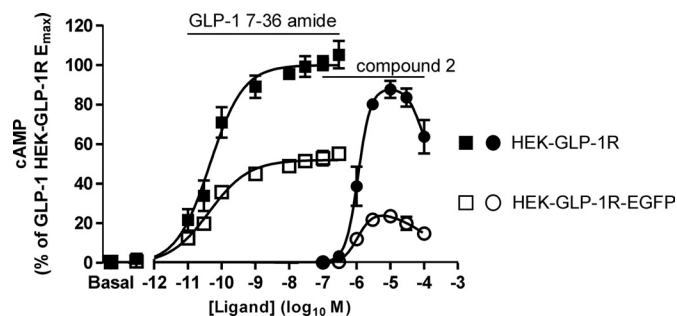
Fig. 9. GLP-1-(7-36) amide- and compound 2-mediated cAMP generation in HEK-GLP-1R cells and cells with stable expression of an EGFP-tagged GLP-1R. A cell line was generated with stable expression of a C-terminally tagged GLP-1R (HEK-GLP-1R-EGFP), and either these cells or HEK-GLP-1R cells were challenged with either GLP-1-(7-36) amide (□ and ■, respectively) or compound 2 (○ and ●, respectively) at the indicated concentrations for 10 min in the presence of IBMX (500 μM). Levels of intracellular cAMP were determined relative to the cellular protein content and are expressed in relation to the maximal response generated by GLP-1-(7-36) amide in HEK-GLP-1R cells. Whenever compound 2 was used, the final concentration of DMSO (vehicle) was 5% (v/v) in all cases. The pEC_{50} values were as follows: HEK-GLP-1R, 10.40 ± 0.27 and 6.00 ± 0.13 for GLP-1-(7-36) amide and compound 2, respectively; HEK-GLP-1R-EGFP, 10.41 ± 0.18 and 6.02 ± 0.03 GLP-1-(7-36) amide and compound 2, respectively. Data are mean ± S.E.M., $n = \geq 3$.

Receptor Internalization. Stable expression of a C-terminal EGFP-tagged hGLP-1R (GLP-1R-EGFP) in HEK-293 cells resulted in a cell line (HEK-GLP-1R-EGFP) with a K_d value for GLP-1-(7-36) amide of -8.98 ± 0.14 $\log_{10}$ M and a B_{max} value of 951 ± 213 fmol/mg protein. In parallel experiments using the HEK-GLP-1R and HEK-GLP-1R-EGFP cell lines, the potencies of GLP-1-(7-36) amide (pEC_{50} values 10.40 ± 0.27 and 10.41 ± 0.18, respectively) and compound 2 (pEC_{50} values 6.00 ± 0.13 and 6.02 ± 0.03, respectively) were not different between the cell lines, although the E_{max} values were lower in the HEK-GLP-1R-EGFP cell line (E_{max} values for GLP-1-(7-36) amide and compound 2 were 53 and 27% of those in the HEK-GLP-1R cell line; Fig. 9).

Confocal imaging of HEK-GLP-1R-EGFP cells revealed intense, continuous plasma membrane fluorescence (Fig. 10a, 0 min). Challenge of cells with GLP-1-(7-36) amide (100 nM) resulted in marked internalization of fluorescence. In the first 10 min, fluorescence aggregated in small discrete patches at the plasma membrane, and this was followed by movement of these puncta into the interior of the cell where they coalesced in discrete regions (Fig. 10a). Quantification of changes in plasma membrane and cytosolic fluorescence indicated that internalization was at a maximum by approximately 30 min (Fig. 10b) and that relatively little fluorescence remained at the cell membrane (Fig. 10, a and b). Over the 60-min period, a very minor amount of internalization occurred in the presence of DMSO [0.1% (v/v); Fig. 10, a and b], but this was not different from cells in buffer alone (data not shown). The GLP-1 receptor antagonist exendin-(9-39) (100 nM) had no impact on the distribution of fluorescence over and above that seen in vehicle-treated cells (Fig. 10, a and b). However, preincubation of cells with exendin-(9-39) (100 nM) for 10 min reduced the rate and extent of internalization mediated by GLP-1-(7-36) amide (100 nM) (Fig. 10, a and b). After addition of compound 2 (10 μM), there was a delay of approximately 10 min before the initiation of detectable internalization, which then progressed at a slower rate

and was less extensive (67%) than that mediated by GLP-1-(7-36) amide (Fig. 10, a and b). Preincubation of cells with exendin-(9-39) (100 nM) for 10 min reduced the rate and extent of internalization mediated by compound 2 (10 μM) to essentially basal levels (Fig. 10, a and b). Coapplication of GLP-1-(7-36) amide (100 nM) and compound 2 (10 μM) resulted in an initial internalization that was similar to that seen in cells treated with GLP-1-(7-36) amide alone (Fig. 10b). However, between 20 and 60 min the extent of internalization was less than that with GLP-1-(7-36) amide alone but still greater than that with compound 2 alone.

Given the ability of exendin-(9-39) to inhibit compound 2-mediated internalization of the GLP-1R-EGFP, we examined whether this capacity to maintain cell surface receptor was responsible for the ability of exendin-(9-39) to enhance compound 2-mediated cAMP generation by the GLP-1R. Initially, we demonstrated that exendin-(9-39) did indeed enhance compound 2-mediated cAMP generation in HEK-GLP-1R-EGFP cells. Thus, exendin-(9-39) had little effect on the potency of compound 2 but increased the E_{max} value from 84 ± 5 to 100 ± 6% of the GLP-1-(7-36) amide response in these cells (Fig. 11a), mimicking the effect observed in HEK-GLP-1R cells. In a membrane assay of cAMP generation, in which regulation of receptor internalization would not contribute to differences in cAMP generation, exendin-(9-39) inhibited cAMP generation in response to a submaximal concentration of GLP-1 and caused a modest but significant increase in the compound 2-mediated response (Fig. 11b).

Discussion

The GLP-1R is a target for the treatment of type 2 diabetes and although peptides can offer high potency agonism, they do not provide ideal therapeutics. The exciting recent identification of small-molecule allosteric (Knudsen et al., 2007) and orthosteric agonists (Chen et al., 2007) provides hope for the development of high-affinity, orally active compounds having the full spectrum of activity at the GLP-1R and clinical applicability. Here, we have examined agonism of 6,7-dichloro-2-methylsulfonyl-3-*N-tert*-butylaminoquinoxaline (compound 2; Knudsen et al., 2007) for functionally important signaling events and compared these with the primary endogenous orthosteric ligand of the GLP-1R, GLP-1-(7-36) amide.

G protein-coupled receptors belonging to family B, for which endogenous ligands are known, couple to $G\alpha_s$, adenylyl cyclase, and cAMP generation. The GLP-1R is no exception and evidence supports such coupling by endogenous or recombinantly expressed receptors in different cells. Although coupling to $G\alpha_{q/11}$ and $G\alpha_i$, has been reported; particularly by recombinant GLP-1Rs (Montrose-Rafizadeh et al., 1999; Hällbrink et al., 2001; Bavec et al., 2003), we show using immunoprecipitation of G proteins that GLP-1-(7-36) amide activates $G\alpha_s$ but not $G\alpha_{q/11}$ or $G\alpha_i$ in our cell line. Furthermore, GLP-1-(7-36) amide robustly increases intracellular cAMP. Compound 2, shown previously to generate cAMP in membrane-based assays with biphasic concentration dependence (Knudsen et al., 2007) also activated $G\alpha_s$ in membranes and generated cAMP in intact cells. The concentration dependence of $G\alpha_s$ activation and cAMP generation in long (90 min) but not short (10 min) assays was biphasic.
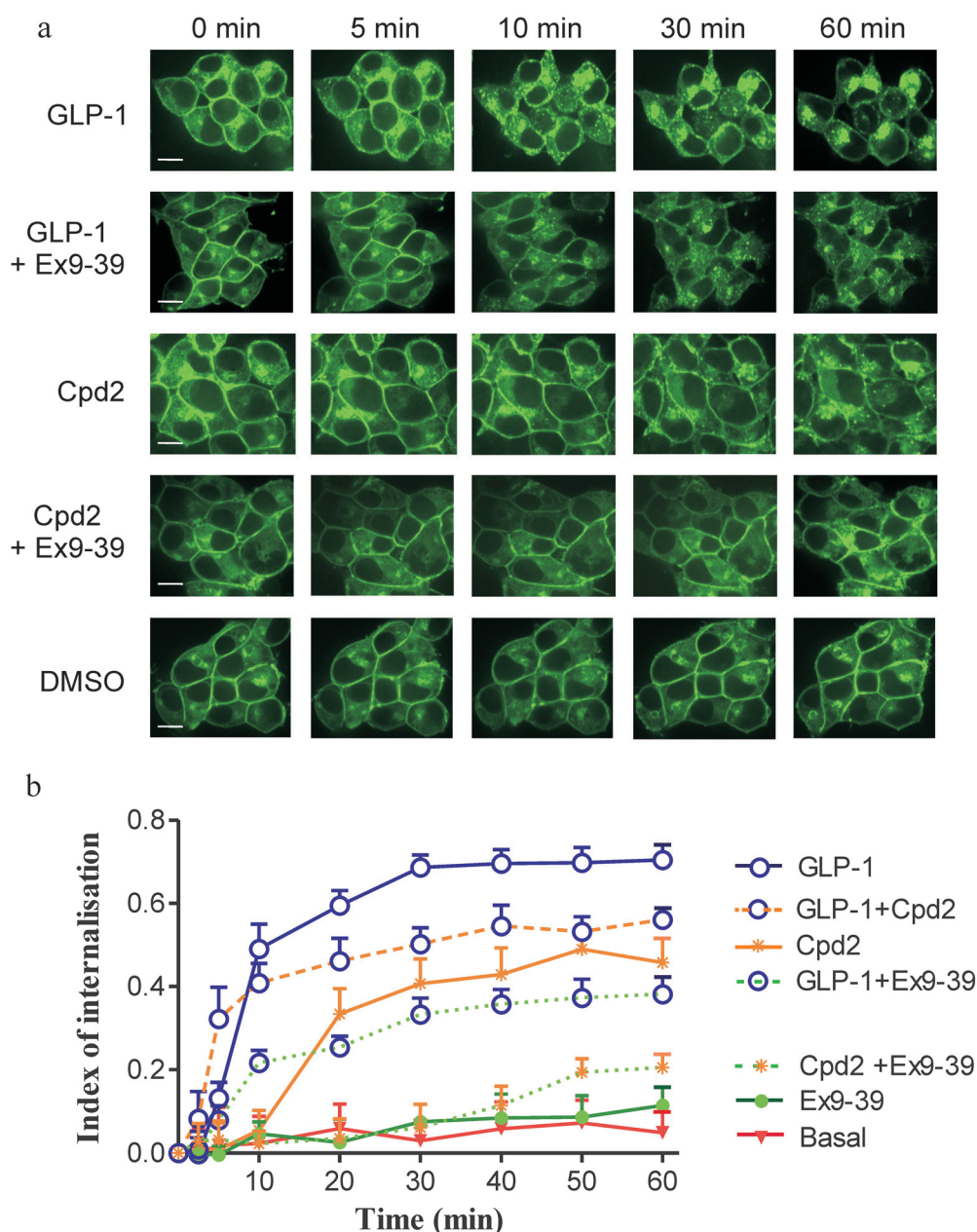
Fig. 10. Agonist-mediated internalization of the GLP-1R. a, HEK-GLP-1R-EGFP were imaged by confocal microscopy over a 60-min period during which time they were challenged with GLP-1-(7-36) amide (GLP-1; 100 nM) in the absence or presence of exendin-(9-39) (Ex9-39; 100 nM), compound 2 (Cpd2; 10 μM) in the absence or presence of exendin-(9-39) (100 nM), GLP-1-(7-36) amide (100 nM), and compound 2 (10 μM; b only), exendin-(9-39) (100 nM; b only), and DMSO [0.1% (v/v); basal] as indicated. Images were taken periodically over the 60-min period and shown here are images representative of three experiments showing the distribution of EGFP fluorescence at 0, 5, 10, 30, and 60 min. Scale bar (in the bottom left of the first image in each row), 5 μm. b, using the procedure described under *Materials and Methods*, an index of internalization was derived from six randomly chosen cells for each condition in each of three independent experiments. Data are mean + S.D., $n = 18$.

Curves of this shape are probably due to adverse effects of compound 2, because in both membranes (Knudsen et al., 2007) and cells (Fig. 5c), higher concentrations inhibit forskolin-mediated cAMP generation. Although estimates may be compromised by adverse effects, data indicate that compound 2 activates $G\alpha_s$ with low potency (4.4 μM) and low efficacy (16% of GLP-1-(7-36) amide) and elevates cAMP with low potency (0.59 μM) but higher efficacy (88% of GLP-1-(7-36) amide). These differences in potency and efficacy may reflect signal amplification. Adverse effects of compound 2 are independent of GLP-1R expression and include effects independent of cell viability, one manifestation of which is a direct effect on receptors. For example, in a 1-h assay at 37°C, 10 μM compound 2 reduced binding of the muscarinic receptor antagonist 1-[N-methyl-³H]scopolamine methyl chloride to muscarinic M_3 receptors stably expressed in HEK-293 cells (27 ± 3% of control; $n = 3$; see Tovey and Willars, 2004 for description of cell line). These adverse effects are a likely

consequence of the chemical nature of compound 2 (Knudsen et al., 2007).

Here, we show that like the endogenous ligand, compound 2 elevates $[Ca^{2+}]_i$ by release from thapsigargin-sensitive intracellular stores, albeit with slower kinetics. Although compound 2 potency and efficacy could not be determined, GLP-1-(7-36) amide elevated $[Ca^{2+}]_i$ and cAMP with similar potency, consistent with other recombinant systems (Wheeler et al., 1993; Widmann et al., 1994; Syme et al., 2006). Ca^{2+} signaling by the GLP-1R reflects an important physiological role and is likely to be a critical property of therapeutics targeting this receptor. Ca^{2+} is key for insulin release from pancreatic β cells where there is a complex interplay between pathways evoking Ca^{2+} responses (Doyle and Egan, 2007; Holst, 2007). GLP-1-mediated Ca^{2+} signaling in β cells includes protein kinase A (PKA)-dependent inhibition of K_{ATP} channels, which at higher glucose concentrations causes mem-
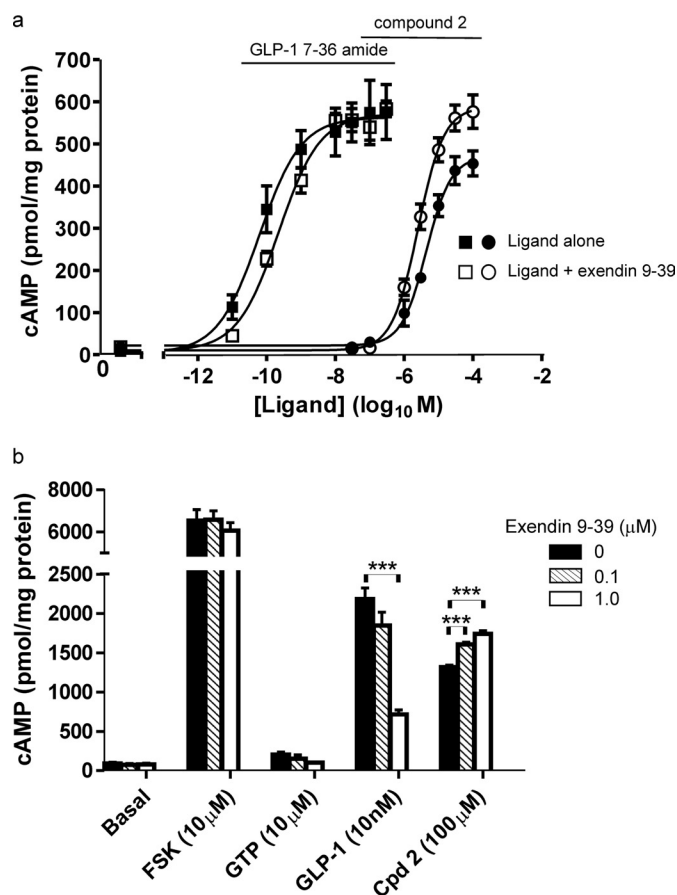
Fig. 11. Enhancement of compound 2-mediated cAMP generation by exendin-(9-39). a, intact HEK-GLP-1R-EGFP cells were pretreated for 10 min with either exendin-(9-39) (100 nM) or vehicle (KHB) in the presence of IBMX (500 μM) before challenge for 5 min with the indicated concentrations of GLP-1-(7-36) amide (■, □) or compound 2 (●, ○) in the continued absence (■, ●) or presence of exendin-(9-39) (□, ○). When compound 2 was used, the final concentration of DMSO (vehicle) was 5% (v/v). Levels of intracellular cAMP were determined relative to the cellular protein content. The pEC_{50} values were as follows: GLP-1-(7-36) amide, 10.20 ± 0.09 and 9.65 ± 0.10 in the absence and presence of exendin-(9-39), respectively; compound 2, 5.36 ± 0.04 and 5.61 ± 0.07 in the absence and presence of exendin-(9-39), respectively. b, membranes were prepared from HEK-GLP-1R cells and unchallenged (basal) or challenged with either forskolin (FSK; 10 μM) or GTP (10 μM). Alternatively, membranes were challenged with either GLP-1-(7-36) amide (10 nM) or compound 2 (Cpd 2; 100 μM). For each of the conditions, membranes were challenged in the presence of IBMX in the absence (0) or presence of exendin-(9-39) (0.1 or 1 μM) as indicated. Reactions were terminated after 5 min at 30°C, and cAMP levels were determined and expressed relative to membrane protein. The concentration of GLP-1-(7-36) amide used (10 nM) was submaximal as 100 nM generated 8742 ± 133 pmol/mg protein cAMP. All data are mean $\pm$ or $+$ S.E.M., $n = \geq 4$. ***, $p < 0.001$ by Dunnett's test after one-way analysis of variance.

brane depolarization and activation of voltage-operated Ca^{2+} channels. In addition, PKA may directly regulate voltage-operated Ca^{2+} channels and K_v channels, enhancing Ca^{2+} entry. Adenylyl cyclase activation also facilitates insulin exocytosis through a PKA-dependent mobilization of intracellular Ca^{2+} stores, an exchange protein directly activated by cyclic AMP-dependent sensitization of ryanodine receptors and/or a PKA-dependent sensitization of inositol trisphosphate receptors (Doyle and Egan, 2007). Furthermore, at low physiological concentrations of GLP-1, insulin-secretion is PKA-independent but Ca^{2+}-dependent (Shigeto et al., 2008). Compound 2 clearly pro-

vokes glucose-dependent insulin release (Knudsen et al., 2007), although the contributions of different Ca^{2+} signaling mechanisms are unknown.

Our data suggest that GLP-1R-mediated responses are not downstream of either $G\alpha_{q/11}$ or $G\alpha_{i/o}$ activation. Although coupling to all G proteins has not been examined, data are at least in line with signaling through $G\alpha_s$ activation. This is consistent with coupling of the endogenous receptor in β-cell lines (Widmann et al., 1994) and the recombinant receptor in some (Widmann et al., 1994) but not all (Wheeler et al., 1993) cell types. Assessment of the involvement of $G\alpha_s$ using CTX treatment was hampered by the ongoing stimulatory effects of the toxin even after 20 to 24 h of treatment. Substantial residual agonist-mediated cAMP generation also highlighted the difficulty of using this toxin to assess the role of $G\alpha_s$ in other signaling events. The precise mechanisms by which GLP-1R activation releases Ca^{2+} from stores after activation by either agonist are unclear. Pretreatment with pertussis toxin had no effect on Ca^{2+} signaling. Furthermore, neither agonist caused accumulation of [^{3}H]inositol phosphates over 30 min against a lithium block of inositol monophosphatase activity (data not shown; see Willars and Nahorski, 1995), indicating an absence of phospholipase C activity. Despite difficulties associated with the use of U73122 (Werry et al., 2003), the lack of effect of this putative phospholipase C inhibitor on Ca^{2+} signaling further supports a lack of its involvement in Ca^{2+} responses.

GLP-1-(7-36) amide-mediated cAMP generation was inhibited by the orthosteric competitive antagonist exendin-(9-39) (Göke et al., 1993; Thorens et al., 1993) with an apparent pA_2 of 7.29 (52 nM). Although greater than the reported K_d value (~1 nM; Thorens et al., 1993), our estimate is from very different conditions in a functional assay without full Schild analysis. Exendin-(9-39) did not inhibit compound 2-mediated cAMP generation, consistent with agonism at an allosteric site (Knudsen et al., 2007), which has been speculated to be a cavity near transmembrane 5 and transmembrane 6 (Lin and Wang, 2009). Compound 2 increases GLP-1 affinity (Knudsen et al., 2007), and it was surprising that compound 2 reduced GLP-1 potency for cAMP generation. Although these data could indicate that compound 2 is a partial agonist at the orthosteric site or an allosteric agonist with negative cooperativity, we believe such interpretation is severely compromised by adverse effects of compound 2, which manifest here as reduced GLP-1 potency. Our data are also inconsistent with the previous report that compound 2 does not influence GLP-1 potency (Knudsen et al., 2007). However, in that study, the potencies of GLP-1 and compound 2 were much higher, consistent with greater levels of receptor expression and therefore much lower levels of compound 2 were used, which may have had rather more limited adverse effects.

Surprisingly, exendin-(9-39) increased the E_{max} of compound 2-mediated cAMP generation in both intact cell and membrane-based assays. Although compound 2 can increase orthosteric agonist affinity (Knudsen et al., 2007), it is unclear how increased efficacy occurs. Exendin-(9-39) may facilitate the stabilization of a more active receptor conformation by compound 2 or protect against the adverse effects of compound 2.

Compared with compound 2, receptor internalization mediated by GLP-1-(7-36) amide was both faster and

greater. The mechanisms underlying GLP-1R internalization are unclear. In HEK-293 and MIN6 cells, internalization is an arrestin-independent, caveolin-mediated process (Syme et al., 2006). However, G protein-coupled receptor kinase-dependent receptor phosphorylation and β-arrestin 2-dependent internalization, presumably via a clathrin-dependent pathway, has been implicated in other cells (Widmann et al., 1995; Jorgensen et al., 2005; Vázquez et al., 2005). Internalization of GLP-1-bound receptors may be important for ligand dissociation and receptor resensitization. Furthermore, for some receptors, internalization is critical for coupling to specific pathways, particularly G protein-independent signaling, which can include the mitogen-activated protein kinases. We have not explored the mechanisms or consequences of internalization here, and it is unclear whether they are identical after activation by allosteric and orthosteric agonists. The observed differences in internalization could reflect partial agonism of compound 2 or differences in receptor occupancy. Thus, although we selected agonist concentrations that were maximal and approximately equally effective on cAMP generation (10-min assay), receptor occupancies may differ. Compound 2 toxicity prevented use of supramaximal concentrations to overcome this problem. Toxicity could also limit internalization, even at lower concentrations, although this is not supported by the ability of GLP-1-(7-36) amide to enhance internalization in the presence of compound 2. Surprisingly, exendin-(9-39) inhibited compound 2-mediated receptor internalization. It is possible that exendin-(9-39) generates a receptor conformation unable to internalize, even in the presence of an allosteric agonist, but this is not associated with reduced signaling. Indeed, exendin-(9-39) enhanced compound 2 efficacy, but this was unrelated to reduced internalization because it was present in membrane cAMP assays. It is unclear whether exendin-(9-39) reduces processes associated with desensitization such as receptor phosphorylation, which would promote signaling and reduce arrestin-dependent internalization.

Thus, compound 2 displays agonism at the GLP-1R that is qualitatively similar to that of the major endogenous ligand GLP-1-(7-36) amide but quantitatively different. Although evidence suggests an allosteric mechanism for compound 2, enhanced efficacy and reduced receptor internalization in the presence of the orthosteric antagonist suggest complex interactions between the allosteric and orthosteric sites. The challenge is to design potent small-molecule GLP-1R agonists in which toxicity does not compromise the therapeutic window and allows full assessment of their pharmacology independent of toxicity.

References

Akam EC, Challiss RA, and Nahorski SR (2001) $G_{q/11}$ and $G_{i/o}$ activation profiles in CHO cells expressing human muscarinic acetylcholine receptors: dependence on agonist as well as receptor-subtype. *Br J Pharmacol* **132:**950–958.

Baggio LL and Drucker DJ (2007) Biology of incretins: GLP-1 and GIP. *Gastroenterology* **132:**2131–2157.

Bavec A, Hällbrink M, Langel U, and Zorko M (2003) Different role of intracellular loops of glucagon-like peptide-1 receptor in G-protein coupling. *Regul Pept* **111:**137–144.

Bleasdale JE, Thakur NR, Gremban RS, Bundy GL, Fitzpatrick FA, Smith RJ, and Bunting S (1990) Selective inhibition of receptor-coupled phospholipase C-dependent processes in human platelets and polymorphonuclear neutrophils. *J Pharmacol Exp Ther* **255:**756–768.

Bradford MM (1976) A rapid and sensitive method for the quantitation of microgram quantities of protein utilizing the principle of protein-dye binding. *Anal Biochem* **72:**248–254.

Brown BL, Albano JD, Ekins RP, and Sgherzi AM (1971) A simple and sensitive saturation assay method for the measurement of adenosine 3′:5′-cyclic monophosphate. *Biochem J* **121:**561–562.

Bundey RA and Nahorski SR (2001) Homologous and heterologous uncoupling of muscarinic M(3) and α_{1B} adrenoceptors to $G\alpha_{q/11}$ in SH-SY5Y human neuroblastoma cells. *Br J Pharmacol* **134:**257–264.

Burford NT, Tobin AB, and Nahorski SR (1995) Differential coupling of m1, m2 and m3 muscarinic receptor subtypes to inositol 1,4,5-trisphosphate and adenosine 3′,5′-cyclic monophosphate accumulation in Chinese hamster ovary cells. *J Pharmacol Exp Ther* **274:**134–142.

Chen D, Liao J, Li N, Zhou C, Liu Q, Wang G, Zhang R, Zhang S, Lin L, Chen K, et al. (2007) A nonpeptidic agonist of glucagon-like peptide 1 receptors with efficacy in diabetic db/db mice. *Proc Nat Acad Sci USA* **104:**943–948.

Dimitriadis GD, Richards SJ, Parry-Billings M, Leighton B, Newsholme EA, and Challiss RA (1991) Beta-adrenoceptor-agonist and insulin actions on glucose metabolism in rat skeletal muscle in different thyroid states. *Biochem J* **278:**587–593.

Doyle ME and Egan JM (2007) Mechanisms of action of glucagon-like peptide 1 in the pancreas. *Pharmacol Ther* **113:**546–593.

Göke R, Fehmann HC, Linn T, Schmidt H, Krause M, Eng J, and Göke B (1993) Exendin-4 is a high potency agonist and truncated exendin-(9-39)-amide an antagonist at the glucagon-like peptide 1-(7-36)-amide receptor of insulin-secreting β-cells. *J Biol Chem* **268:**19650–19655.

Hällbrink M, Holmqvist T, Olsson M, Östenson CG, Efendic S, and Langel U (2001) Different domains in the third intracellular loop of the GLP-1 receptor are responsible for $G\alpha_s$ and $G\alpha_i/G\alpha_o$ activation. *Biochim Biophys Acta* **1546:**79–86.

Heding A, Elling CE, and Schwartz TW (2002) Novel method for the study of receptor Ca^{2+} signalling exemplified by the NK1 receptor. *J Recept Signal Transduct Res* **22:**241–252.

Holst JJ (2007) The physiology of glucagon-like peptide 1. *Physiol Rev* **87:**1409–1439.

Holst JJ, Orskov C, Nielsen OV, and Schwartz TW (1987) Truncated glucagon-like peptide I, an insulin-releasing hormone from the distal gut. *FEBS Lett* **211:**169–174.

Holz GG 4th, Kühtreiber WM, and Habener JF (1993) Pancreatic beta-cells are rendered glucose-competent by the insulinotropic hormone glucagon-like peptide-1(7-37). *Nature* **361:**362–365.

Jorgensen R, Martini L, Schwartz TW, and Elling CE (2005) Characterization of glucagon-like peptide-1 receptor β-arrestin 2 interaction: a high-affinity receptor phenotype. *Mol Endocrinol* **19:**812–823.

Kenakin T (2004) *A Pharmacology Primer: Theory, Application, and Methods*, Elsevier Academic Press, San Diego, CA.

Kieffer TJ, McIntosh CH, and Pederson RA (1995) Degradation of glucose-dependent insulinotropic polypeptide and truncated glucagon-like peptide 1 in vitro and in vivo by dipeptidyl peptidase IV. *Endocrinology* **136:**3585–3596.

Knudsen LB, Kiel D, Teng M, Behrens C, Bhumralkar D, Kodra JT, Holst JJ, Jeppesen CB, Johnson MD, de Jong JC, et al. (2007) Small-molecule agonists for the glucagon-like peptide 1 receptor. *Proc Natl Acad Sci USA* **104:**937–942.

Lin F and Wang R (2009) Molecular modeling of the three-dimensional structure of GLP-1R and its interactions with several agonists. *J Mol Model* **15:**53–65.

Meier JJ and Nauck MA (2005) Glucagon-like peptide 1 (GLP-1) in biology and pathology. *Diabetes Metab Res Rev* **21:**91–117.

Mentlein R, Gallwitz B, and Schmidt WE (1993) Dipeptidyl-peptidase IV hydrolyses gastric inhibitory polypeptide, glucagon-like peptide-1(7-36)amide, peptide histidine methionine and is responsible for their degradation in human serum. *Eur J Biochem* **214:**829–835.

Montrose-Rafizadeh C, Avdonin P, Garant MJ, Rodgers BD, Kole S, Yang H, Levine MA, Schwindinger W, and Bernier M (1999) Pancreatic glucagon-like peptide-1 receptor couples to multiple G proteins and activates mitogen-activated protein kinase pathways in Chinese hamster ovary cells. *Endocrinology* **140:**1132–1140.

Orskov C, Rabenhøj L, Wettergren A, Kofod H, and Holst JJ (1994) Tissue and plasma concentrations of amidated and glycine-extended glucagon-like peptide I in humans. *Diabetes* **43:**535–539.

Reimann F, Ward PS, and Gribble FM (2006) Signaling mechanisms underlying the release of glucagon-like peptide 1. *Diabetes* **55 (Suppl 2):**S78–S85.

Seidel MG, Klinger M, Freissmuth M, and Höller C (1999) Activation of mitogen-activated protein kinase by the A(2A)-adenosine receptor via a rap1-dependent and via a p21(ras)-dependent pathway. *J Biol Chem* **274:**25833–25841.

Shigeto M, Katsura M, Matsuda M, Ohkuma S, and Kaku K (2008) Low, but physiological, concentration of GLP-1 stimulates insulin secretion independent of the cAMP-dependent protein kinase pathway. *J Pharmacol Sci* **108:**274–279.

Syme CA, Zhang L, and Bisello A (2006) Caveolin-1 regulates cellular trafficking and function of the glucagon-like peptide 1 receptor. *Mol Endocrinol* **20:**3400–3411.

Thorens B, Porret A, Bühler L, Deng SP, Morel P, and Widmann C (1993) Cloning and functional expression of the human islet GLP-1 receptor. Demonstration that exendin-4 is an agonist and exendin-(9-39) an antagonist of the receptor. *Diabetes* **42:**1678–1682.

Tovey SC and Willars GB (2004) Single-cell imaging of intracellular Ca^{2+} and phospholipase C activity reveals that RGS 2, 3 and 4 differentially regulate signaling via the $G\alpha_{q/11}$-linked muscarinic M_3 receptor. *Mol Pharmacol* **66:**1453–1464.

Vázquez P, Roncero I, Blázquez E, and Alvarez E (2005) The cytoplasmic domain

close to the transmembrane region of the glucagon-like peptide-1 receptor contains sequence elements that regulate agonist-dependent internalisation. *J Endocrinol* **186:**221–231.

Werry TD, Wilkinson GF, and Willars GB (2003) Cross talk between P2Y$_2$ nucleotide receptors and CXC chemokine receptor 2 resulting in enhanced Ca^{2+} signalling involves enhancement of phospholipase C activity and is enabled by incremental Ca^{2+} release in human embryonic kidney cells. *J Pharmacol Exp Ther* **307:**661–669.

Wheeler MB, Lu M, Dillon JS, Leng XH, Chen C, and Boyd AE 3rd (1993) Functional expression of the rat glucagon-like peptide-I receptor, evidence for coupling to both adenylyl cyclase and phospholipase-C. *Endocrinology* **133:**57–62.

Widmann C, Bürki E, Dolci W, and Thorens B (1994) Signal transduction by the cloned glucagon-like peptide-1 receptor: comparison with signaling by the endogenous receptors of beta cell lines. *Mol Pharmacol* **45:**1029–1035.

Widmann C, Dolci W, and Thorens B (1995) Agonist-induced internalization and recycling of the glucagon-like peptide-1 receptor in transfected fibroblasts and in insulinomas. *Biochem J* **310:**203–214.

Willars GB and Nahorski SR (1995) Quantitative comparisons of muscarinic and bradykinin receptor-mediated Ins (1,4,5)P$_3$ accumulation and Ca^{2+} signalling in human neuroblastoma cells. *Br J Pharmacol* **114:**1133–1142.

Address correspondence to: Dr. Gary B. Willars, Department of Cell Physiology and Pharmacology, Maurice Shock Medical Sciences Building, University of Leicester, University Rd., Leicester, LE1 9HN, UK. E-mail: gbw2@le.ac.uk